KINETICS OF FRONTS OF THE DEFORMATION PHASE TRANSFORMATION IN NITINOL

Prof. dr. phys.-mat. sci. Danilov V.[1,2 a], Cand. phys.-mat. sci. Gorbatenko V.[1 b],
Prof. dr. phys.-mat. sci. Zuev L.[1,3 c], Cand. phys.-mat. sci. Orlova D.[1,2 d]
Institute of Strength Physics and Material Science Siberian Branch of Russian Academy of Sciences[1],
Tomsk Polytechnic University[2], Tomsk State University[3]

[a]dvi@ispms.tsc.ru, [b]gvv@ispms.tsc.ru, [c]lbz@ispms.tsc.ru, [d]dvo@ispms.tsc.ru

Abstract: *In this study, we investigated the localization of the macroscopic deformation during tensile test of nitinol at room temperature. The specimens were fully austenitic and therefore, the martensitic phase transition under deformation had place. It is established that the deformation phase transformation is realized by the formation and motion of fronts of localized deformation. Fronts moves at constant velocities and annihilated at the meeting. The velocities of their movement are determined by crosshead velocity and the duration of stress plateau. In this respect, the behavior of the phase-transition fronts is completely similar to the kinetics of the Lüders bands fronts observed in mild steel, but distinctive feature of this phenomenon is that the level of localization of the deformation at the phase transition front is an order of magnitude smaller than at the front of the Lüders band. In addition, the phase transition front has a more complex structure than the front of the Lüders band. These features of the kinetics and morphology of the transformation front lead to the fact that its motion takes place under hardening conditions, and inclined strain plateau is observed on the deformation curve.*

KEYWORDS*: LOCALIZED PLASTIC DEFORMATION, LÜDERS BANDS, NITINOL, DEFORMATION PHASE TRANSFORMATION, FRONTS OF PHASE TRANSFORMATION*

1. Introduction

At the initial stages of plastic deformation, a macroscopic heterogeneity of the plastic flow known as Lüders band (LB) is observed in some materials. Investigation of this phenomenon has received a new impetus owing to development of modern methods for recording and analysis of strain distribution in loaded objects [1-3]. Processes of LB formation in iron, copper, magnesium, etc. based polycrystalline alloys, where plastic flow at the micro level is realized by dislocation sliding, were studied in detail [2, 4, 5]. Study of Lüders band fronts kinetics and morphology, both at their generation and propagation, is of special interest. It has now been established that deformation heterogeneity in the form of LB is observed in single crystals, too. Moreover, deformation at the microscopic level is not necessarily presented by dislocation sliding. Movement of localized deformation fronts was recorded and studied in nickel bronze single crystals, twinning austenitic manganese steel single crystals and Ni_3Mn ordered alloy [6]. In all these cases deformation curves commonly featured a yield plateau.

It is possible to suggest that the applied strain dependence on a material with yield drop and yield plateau is mutually consistent with the formation of localized deformation space-time structure in the form of switching autowave [7]. In this case, the micromechanism of plastic flow shall not play a decisive role, and occurrence of such feature as the yield plateau on the deformation curve may be an attribute of macroscopic deformation localization in the form of mobile fronts.

On the other hand, deformation curves with yield plateaus are typical of materials in which plastic flow at the micro level occurs due to phase transformation, like in nitinol, for instance. Phase transformation front in nitinol deformation was captured [8], however, the morphology and kinetics of these fronts were not studied. All those items are subjects of this paper.

2. Material and experimental procedures

The investigations declared were carried out using nitinol composed of 55.76 wt. % Ni + 44.24 wt. % Ti. The tensile specimen was flat dog-bone specimen with a 40 mm of the gauge length, 6 mm width and 1 mm thickness. Prepared specimens were annealed in a salt-bath furnace at 450 °C and cooled down in water. After the heat treatment, nitinol of this composition demonstrated the following characteristics.

1. Temperature of cubic (B2) to rhombohedral (R) phase transition, T_R = +31°C;
2. Start temperature of martensitic rhombohedral (R) to monoclinic (B19') phase transition, M_s = -13°C;
3. End temperature of martensitic rhombohedral (R) to monoclinic (B19') phase transition, M_f = -54°C;
4. Start temperature of reverse monoclinic (B19') to cubic (B2) phase transition, A_S = +10°C;
5. End temperature of reverse monoclinic (B19') to cubic (B2) phase transition, A_f = +24°C.

Thus, the specimens were in R phase at room temperature and were supposed to have R → B19' deformation phase transition at uniaxial tension. When the load is removed, the reverse B19' → B2 transition is not possible without cooling; therefore, superelasticity diagram at room temperature can't be obtained. However, it is fairly suitable for studying macroscopic features of deformation-induced phase transformation kinetics and morphology. The specimens were tested at a constant rate of V_{mach} = 3.3×10^{-3} mm/s.

Deformation localization fronts were visualized using digital image correlation (DIC) method [1]. It was implemented by recording and digitizing a sequence of speckle images at a 10 Hz frequency. A flat grid of 1×1 mm or 0.5×0.5 mm square cells is applied on each recorded image, and displacements of grid nodes for 6 s time shift are determined that corresponds to the absolute displacement by 1 pixel, at most. The measured field of displacement vectors, $\boldsymbol{r}$, was numerically differentiated by coordinates that allows determination of distortion tensor δ_{ij}[1] components for the flat case [8]. In this study, distribution of local elongations ε_{xx} and local rotations ω_z is analyzed.

3. Results and discussion

The analysis of the stress-strain diagram curves of the above samples showed that their initial parts contain a well-defined linear section in the range of 0.022 < ε < 0.058 with a minor strengthening

[1] $\delta_{ij} = \begin{vmatrix} \varepsilon_{xx} & \varepsilon_{xy} \\ \varepsilon_{yx} & \varepsilon_{yy} \end{vmatrix} + \begin{vmatrix} 0 & \omega_{xy} \\ \omega_{yx} & 0 \end{vmatrix}$, were $\varepsilon_{xx} = \frac{\partial u}{\partial x}$ – local elongations, $\varepsilon_{xy} = \varepsilon_{yx} \frac{1}{2}\left(\frac{\partial v}{\partial x} + \frac{\partial u}{\partial y}\right)$ – local shears, $\varepsilon_{yy} = \frac{\partial v}{\partial y}$ – local contractions,

$\omega_{xy} = \omega_{yx} = \omega_z = \frac{1}{2}\left(\frac{\partial v}{\partial x} - \frac{\partial u}{\partial y}\right)$ – local rotations, u and v – components of displacement vector $\boldsymbol{r}$ Along the extension axis and perpendicular to it, respectively

θ_I = 816 MPa equal to 2 to 4% of the material shear modulus (see fig. 1).

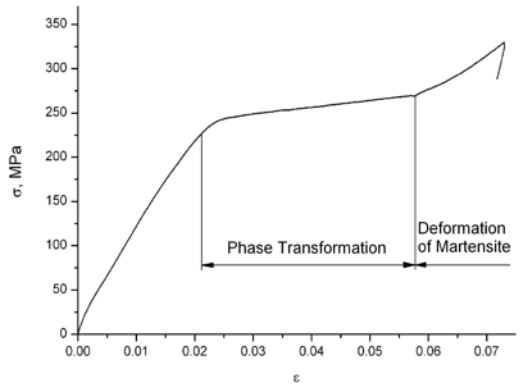

Fig. 1. Nitinol specimen stress-strain diagram at room temperature

It is obvious that the deformation-induced phase transformation takes place at this section, therefore, it was selected for deformation localization zones DIC visualization attempt. By sensitivity to displacements, this method is comparable with the classical double-exposure speckle photography [9]. However, both these methods have insufficient spatial and temporal resolution, which prevented us from studying deformation-induced transformation band formation process and transformation front morphology details. Nevertheless, the fronts proper are fairly well revealed (Figs. 2, 3). In all studied cases, two transformation bands were formed at ends of the specimen. Each transformation front is characterized by a maximum of local elongations ε_{xx} (Fig. 2). Mobile band fronts moved towards each other and annihilated. The incline of both fronts to axis of elongation is ≈ 60°, on average. Front velocities are the same, constant and equal to 0.044 mm/s. This correlates well with the relationship (1) previously determined for LBs front velocities in steels [10].

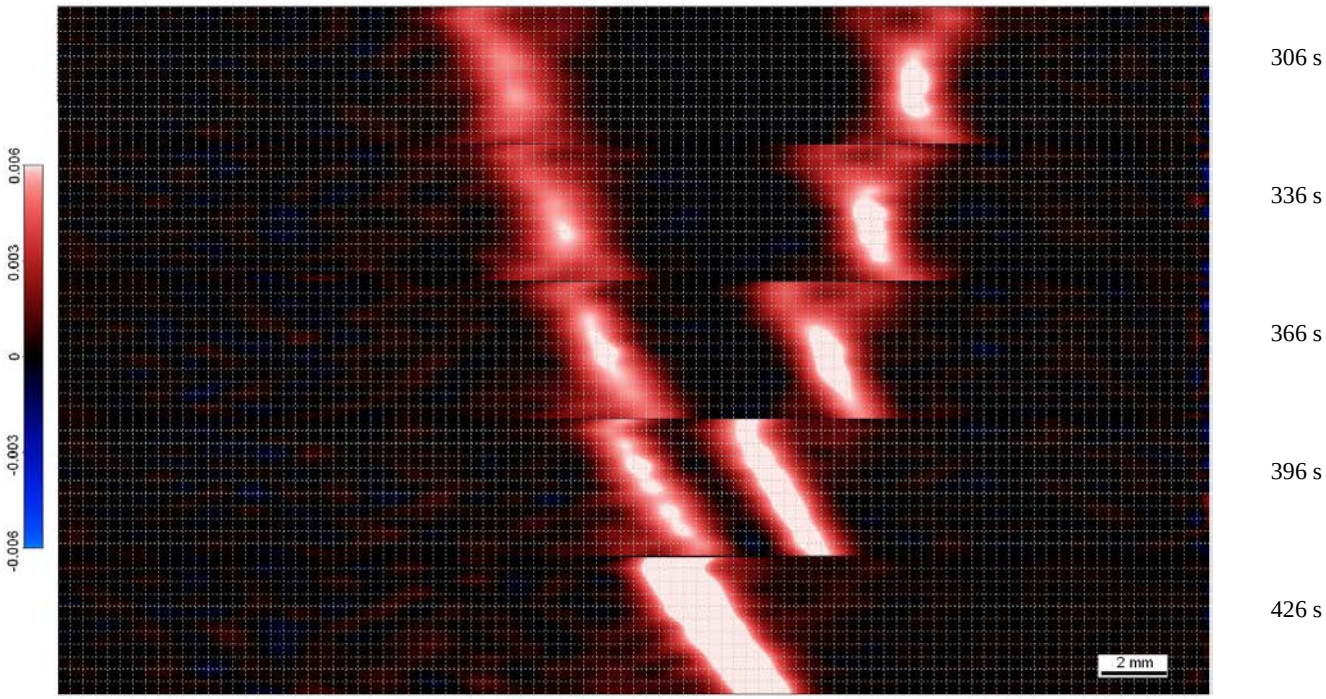

Fig. 2. Movement of deformation-induced phase transformation fronts in nitinol. Times are indicated from the start of recording (see Fig. 1).

$$\sum \left| V_f^{(i)} \right| = \frac{V_{mach}}{\varepsilon_{pl}}, \qquad (1)$$

were $\left| V_f^{(i)} \right|$ - is velocity modulus for each of the moving fronts; ε_{pl} is yield plateau length in deformation units.

It is important to note that characteristic changes in distortion tensor rotation component ω_z are associated with transformation fronts (Fig. 3). The front itself is represented by a negative rotation which spatially coincides with the local elongations maximum. As the fronts approach, the amplitude of this rotation increases and reaches its maximum when the fronts meet (annihilate). Two local areas of positive rotations are located ahead and behind each front during movement. As the fronts come closer, the entire space between them is occupied by the positive rotation area. After annihilation of the fronts, i.e. after completion of the deformation-induced phase transformation, deformation localization at the macroscopic level is stopped, and positive and negative rotations disappear. A short-term stress decay, similar to that occurring when LB fronts meet in low-carbon steel, is observed on the deformation curve [10]. Plastic deformation of the formed B19' martensite occurs rather homogeniously, with the strain-hardening coefficient $\theta_{II} \approx 4$ GPa.

4. Conclusion

Based on the data presented, it can be asserted that deformation-induced phase transformation in nitinol does develop in a manner similar to LB propagation in iron-carbon alloys. Mobile transformation fronts are formed, where the entire deformation is localized. The phase transformation fronts orientation and velocities follow patterns established for LB fronts. Like LB fronts, phase transformation fronts annihilate when they meet.

However, some distinctive features were also identified. The degree of deformation localization at phase transition fronts is an order of magnitude lower than at the LB front, therefore, they are not detected by digital statistical speckle photography method [3, 10]. Not only elongation is localized at the deformation-induced phase transformation front. Movement of the front goes with meaningful rotation processes. As a result, transformation can't take place at constant stress, and the load curve features a inclined yield plateau. This may be explained by the fact that transformation at the microscopic level follows martensitic mechanism which is known to be self-locking due to internal stress occurrence [11].

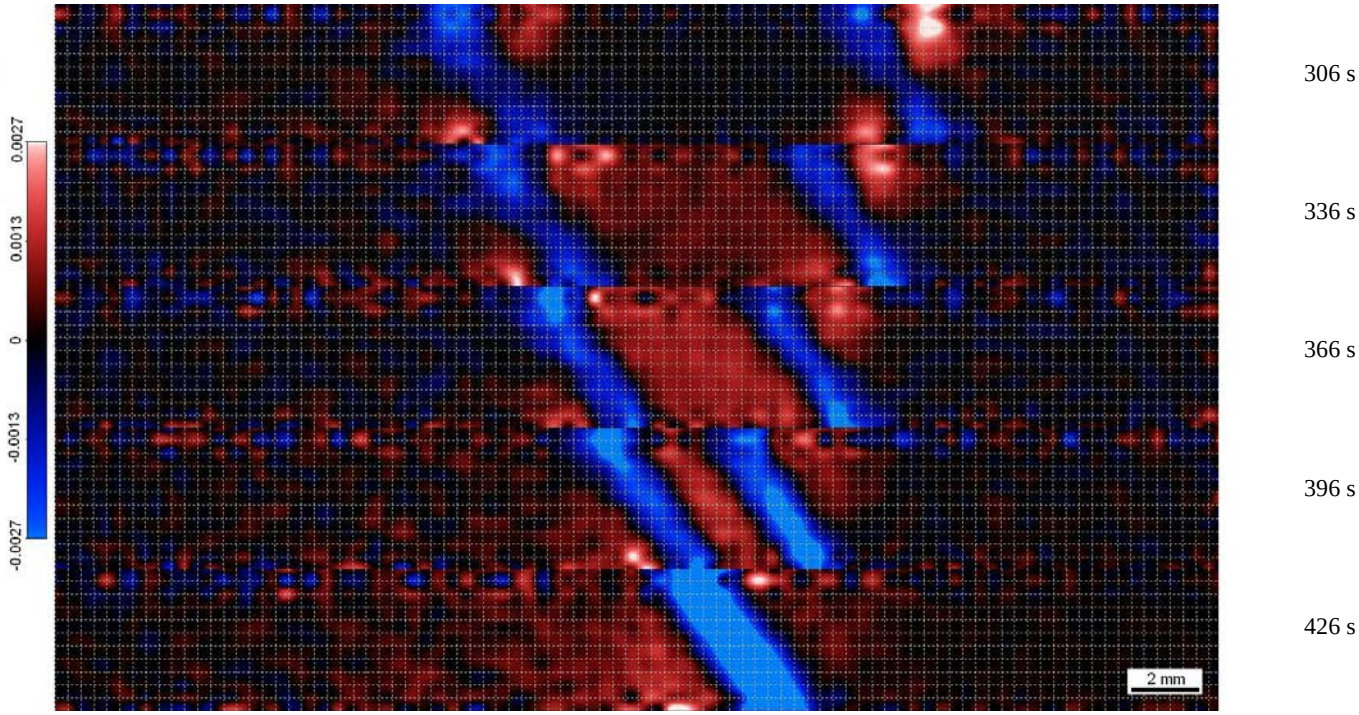

Fig. 3. Changes in distortion tensor rotation component at the deformation-induced phase transformation fronts

Acknowledgments

The work was carried out within the framework of the Program of Fundamental Scientific Research Russian State academies of sciences for 2013-2020.

References

[1] Sutton M.A., Wolters W.J.,. Peters W.H, Ranson W.F., and McNeill S.R. Determination of displacements using an improved digital correlation method. – Image and Vision Computing, vol. 1(3), 1983, pp. 133–139.

[2] Avril S., Pierron F., Sutton M. A., Yan J. Identification of elasto-visco-plastic parameters and characterization of Lüders behavior using digital image correlation and the virtual fields method. – Mechanics of Materials, vol. 40, 2008, pp. 729–742 .

[3] Zuev L.B., Gorbatenko V.V., Pavlichev K.V. Elaboration of speckle photography techniques for plastic flow analyses. – Measurement Science and Technology, vol. 21, No. 16, 2010, 054014-18.

[4] Plekhov O.A., Naimark O.B., Saintier N., Palin-Luc T. Elastic-plastic transition in iron: Structural and thermodynamic features. – Technical Physics, vol. 54, 2009, pp. 1141-1146.

[5] Wang X.G., Wang L.,. Huang M.X. Kinematic and thermal characteristics of Luders and Portevin-Le Chatelier bands in a medium Mn transformation-induced plasticity steel. – Acta Materialia, vol. 124, 2017, pp. 17-29.

[6] Zuev L.B., Danilov V.I. A self-excited wave model of plastic deformation in solids – Philosophical magazine, vol. 79, No. 1, 1999, pp. 43-57.

[7] Zuev L.B. Chernov-Luders and Portevin-Le Chatelier deformations in active deformable media of different nature. – Journal of Applied Mechanics and Technical Physics, vol. 58, No. 2, 2017, pp. 328-334.

[8] Zuev L., Kartashova N., Danilov V., Chumlyakov Yu., Poletika T. The patterns of localization of deformation in a material with plasticity of transformation (single crystalline TiNi). – Technical Physics, vol. 41, No. 11, 1996, pp. 1189–1192.

[9] Jones R., Wykes C. Holographic and Speckle Interferometry. – Cambridge: Cambridge Univ. Press, 1983, 328 p.

[10] Danilov V., Gorbatenko V., Zuev L., Autowaves of localized plastic deformation on the yield plateau and on the work hardening stage. – Materials science. Non-equilibrium phase transformation, vol. 3, 2016, pp. 21-24.

[11] Nishiyama Z. Martensitic Transformation. – London, New York: Academic Press, 1978, 480 p.